Planar cyclotron motion in unidirectional superlattices defined by strong magnetic and electric fields: Traces of classical orbits in the energy spectrum

S. D. M. Zwerschke
Max-Planck-Institut für Festkörperforschung, Heisenbergstraße 1, D-70569 Stuttgart, Germany

A. Manolescu
Institutul Naţional de Fizica Materialelor, C.P. MG-7 Bucureşti-Măgurele, Romania

R. R. Gerhardts
Max-Planck-Institut für Festokörperforschung, Heisenbergstraße 1, D-70569 Stuttgart, Germany
(Received 14 December 1998)

We compare the quantum and the classical description of the two-dimensional motion of electrons subjected to a perpendicular magnetic field and a one-dimensional lateral superlattice defined by spatially periodic magnetic and electric fields of large amplitudes. We explain in detail the complicated energy spectra, consisting of superimposed branches of strong and of weak dispersion, by the correspondence between the respective eigenstates and the ''channeled'' and ''drifting'' orbits of the classical description. [S0163-1829(99)04732-3]

I. INTRODUCTION

In the last decade there has been a constant interest in the transport properties of the periodically modulated two-dimensional electron gas (2DEG). In particular, in the presence of a lateral modulation of a one-dimensional character the resistivity may be strongly anisotropic, which essentially reflects the anisotropy of the electronic states. Two types of modulations can be achieved in the experimental devices: electrostatic potential modulations[1–4] and, more recently, magnetic-field modulations.[5–8] Weak modulations of both types lead already to pronounced magnetoresistance effects in the presence of an average magnetic field B_0 applied perpendicular to the 2DEG. These effects occur at low and intermediate B_0 values, well below the magnetic quantum regime where Shubnikov–de Haas oscillations appear. At very small values of B_0 a pronounced positive magnetoresistance is observed, followed at intermediate B_0 values by the ''Weiss oscillations'' due to commensurability effects. Both effects are adequately understood within a classical transport calculation based on Boltzmann's equation, and can be traced back to the predominance of different types of classical trajectories.[9–11]

The positive magnetoresistance is understood as caused by ''channeled orbits'' which exist if the modulation is sufficiently strong or, equivalently, the average magnetic field is sufficiently small. For electric modulation they occur near the minima of the modulation potential (''open'' orbits[10]), and for magnetic modulation near the lines of vanishing total magnetic field (''snake'' orbits[12]). They are always confined within a single period of the modulation, which we choose in x direction. They are wavy trajectories allowing for fast motion of electrons with velocities within small angles around the direction of translational invariance (y direction). These channeled orbits occur in addition to the ''drifting orbits,'' which are self-intersecting trajectories with loops (along each of which the direction of the velocity changes by 2π), so that usually a low drift velocity in the y direction results. For sufficiently small B_0, drifting orbits may extend over many periods of the modulation. At sufficiently large B_0 (sufficiently small modulation amplitudes) only the drifting orbits survive. The ''Weiss oscillations'' manifest a commensurability effect depending on the ratio of the extent of drifting orbits (at the Fermi energy) and the modulation period. With increasing modulation strength, the positive magnetoresistance becomes more pronounced and extends to larger B_0 values, suppressing progressively the low-B_0 Weiss oscillations.[10] This effect is well understood within the classical calculation,[11] if both types of trajectories are adequately included, and it has recently also been obtained by a quantum calculation for a strong modulation.[13]

A qualitatively new type of magnetoresistance effect has recently been observed by Ye *et al.*[14] on samples with an extremely strong magnetic modulation. Samples with a surface array of ferromagnetic microstrips were measured in tilted magnetic fields, so that the applied magnetic field had a large component parallel to the surface, producing a large magnetization of the ferromagnetic strips, while only the small perpendicular component determined the average magnetic field B_0 in the 2DEG. In this way a huge positive magnetoresistance with superimposed Shubnikov–de Haas-like oscillations was obtained at low values of the average magnetic field, at which no magnetic quantum effects should be expected for weak modulation.[14] It rather seems that the quantum oscillations are induced by the large-amplitude periodic magnetic modulation field. Such conditions require a quantum transport theory and, as a first step, the understanding of the quantum electronic states of a 2DEG with a strong magnetic modulation. This is the motivation of the present work.

Channeled and drifting quantum states in linearly varying magnetic field are already discussed by other authors.[12,15] The Schrödinger equation for periodic magnetic fields alternating in sign has been solved previously, but only for the case when the average field is zero.[16] In the present paper we shall study the quantum electronic states in strong periodic

 ©1999 The American Physical Society

magnetic fields with a nonvanishing average and compare it with the case of a strong electric modulation. In both situations rather complicated energy spectra are obtained, with striking qualitative similarities and quantitative differences. For the case of strong electric modulation, such a complicated energy spectrum has recently been published,[13] but without an attempt at explanation. We will demonstrate in this paper that a close comparison with classical motion leads to a detailed and intuitive understanding of these spectra and the corresponding eigenstates.

In Sec. II we start with some general remarks on the relation between quantum and classical description of the 2D electron motion in one-dimensional (1D) lateral superlattices, and we introduce suitable reduced units. In Sec. III we focus on the effect of a simple harmonic magnetic modulation of arbitrary strength. In Sec. IV we include an electric modulation, which requires a somewhat different analytical procedure. The inclusion of electric modulation seems also necessary from the experimental point of view, since the ferromagnetic strips on the sample surface introduce a periodic stress field in the sample, which acts as an electric modulation on the 2DEG. Finally, in Sec. V we summarize the essential features derived in the paper and extend the discussion beyond the model of simple harmonic modulations. Some of the present results have been recently published in a preliminary form.[17]

II. GENERAL REMARKS

We consider a (noninteracting) 2DES in the x-y plane subjected to a magnetic field with z component $B_z(x)=B_0+B_m(x)$ and an electrostatic field in x direction leading to a potential energy $U(x)$. Our aim is a close comparison of the classical and the quantum description of the electron motion (in terms of orbits and wave functions, respectively) in such fields, especially in the case that $U(x)$ and $B_m(x)$ are periodic in x with the same period a and vanishing average values.

To evidence the translation invariance in y direction in the (either classical or quantum) Hamiltonian

$$H=\frac{1}{2m}(\mathbf{p}+e\mathbf{A})^2+U, \tag{1}$$

we describe $B_z(x)$ by an x-dependent vector potential $\mathbf{A}(x)=A(x)\,\mathbf{e}_y$ with $A(x)=xB_0+A_m(x)$ and $A_m(x)=\int_0^x dx' B_m(x')$. Then y is a cyclic variable and the canonical momentum p_y is conserved, and one obtains a (one-dimensional) effective Hamiltonian $H(X_0)=p_x^2/2m+V(x;X_0)$. For $B_0\neq 0$, the effective potential can be written

$$V(x;X_0)=\frac{m}{2}\omega_0^2\left(x-X_0+\frac{A_m(x)}{B_0}\right)^2+U(x), \tag{2}$$

where $X_0=-p_y/eB_0$ is the center coordinate of the effective potential and $\omega_0=eB_0/m$ is the cyclotron frequency, both in the absence of modulation.

In the quantum description, the reduction to a one-dimensional problem is achieved by the product ansatz $\Psi_{n,X_0}(x,y)=L_y^{-1/2}\exp(ip_y y/\hbar)\psi_{n,X_0}(x)$ for the energy eigenfunctions, where L_y is a normalization length, and the discrete quantum number $n=0,1,2,\ldots$ counts the nodes of the reduced wave function $\psi_{n,X_0}(x)$. If $U(x)$ and $A_m(x)$ are bounded, the $\psi_{n,X_0}(x)$ drop Gaussian-like for $|x|\to\infty$, and for a fixed value of the quasicontinuous quantum number X_0 the energy spectrum $E_n(X_0)$ is discrete.

In the classical description, we use the equation $mv_y=p_y+eA(x)$, which may also be derived directly from Newton's equation, to eliminate the velocity v_y. The effective motion in x direction is determined by $H(X_0)=E$. Similar to the wave functions, the orbits for given constants of motion, X_0 and E, are bounded in the x direction; however, the energy E is a continuous variable. For a given $E=E_F$, each position x [with $U(x)<E_F$] is the turning point of two orbits which are characterized by the center coordinates[11]

$$X_0^{\pm}(x)=x+\frac{A_m(x)}{B_0}\pm R_0\sqrt{1-\frac{U(x)}{E_F}}, \tag{3}$$

obtained from $H(X_0)=E_F$ for $v_x=p_x/m=0$. Here $R_0=v_F/\omega_0$ is the cyclotron radius of electrons moving with energy $E_F=mv_F^2/2$ in the magnetic field B_0. For given E_F and X_0, orbits exist in intervals in which $X_0^-(x)\leqslant X_0\leqslant X_0^+(x)$ holds. This allows a convenient classification of the possible orbits at fixed energy E_F and for varying X_0.[11] Of course, the same classification can also be done by directly investigating the effective potential. This may be preferred if one is interested in orbits at different energies but the same X_0.

The calculation of the orbits is a simple textbook problem, but must in general be done numerically. In accordance with the translational symmetry of the problem, we will in the following not distinguish orbits which differ only by a rigid shift in the y direction. If an electron is at time t_i at position (x_i,y_i) on an orbit characterized by the constants of motion E_F and X_0, with turning points x_l and x_r ($x_l<x_i<x_r$), it moves toward one of the turning points so that at time

$$t(x;X_0,E_F)=t_i+\int_{x_i}^{x}\frac{dx'}{|v_x(x';X_0,E_F)|} \tag{4}$$

it is at position $(x,y(x;X_0,E_F))$, with

$$y(x;X_0,E_F)=y_i+\int_{x_i}^{x}\frac{v_y(x';X_0)}{v_x(x';X_0,E_F)}dx', \tag{5}$$

where

$$|v_x(x;X_0,E_F)|=v_F\sqrt{1-V(x;X_0)/E_F}$$
$$=\omega_0\sqrt{[X_0^+(x)-X_0][X_0-X_0^-(x)]}$$

and

$$v_y(x;X_0)=(\omega_0/2)[X_0^+(x)+X_0^-(x)-2X_0].$$

If at one of the turning points x_l or x_r, where $v_x(x;X_0,E_F)=0$, the derivative $\partial V(x;X_0)/\partial x$ vanishes, we call this turning point and this orbit ''critical.'' At critical turning points the integrals (4) and (5) diverge, so that the critical orbits there asymptotically approach straight lines parallel to the y axis. For noncritical orbits the integrals (4) and (5) converge as x approaches the turning points, and the total orbit can be composed out of right-running ($v_x>0$) and left-running

($v_x<0$) pieces with finite traverse time $T(X_0,E_F)=\int_{x_l}^{x_r}dx/|v_x(x;X_0,E_F)|$. The probability density of finding the electron at position x is

$$W(x;X_0,E_F)=1/[T(X_0,E_F)|v_x(x;X_0,E_F)|].$$

This is the classical analog to $|\psi_{n,X_0}(x)|^2$.

If $U(x)=U(x+a)$ and $B_m(x)=B_m(x+a)$ are periodic with period a, as we will assume in the following, the effective potential, Eq. (2), has the symmetry $V(x+a;X_0+a)=V(x;X_0)$. As a consequence, the energy spectrum is also periodic, $E_n(X_0+a)=E_n(X_0)$, and can be restricted to the ''first Brillouin zone'' $0\leqslant X_0\leqslant a$. The eigenfunctions can be taken to satisfy $\psi_{n,X_0+a}(x)=\psi_{n,X_0}(x-a)$. The corresponding classical symmetry is that an orbit characterized by E_F and X_0+a differs from that characterized by E_F and X_0 only by a rigid shift of amount a in the x direction.

The dispersion of the energy bands $E_n(X_0)$ implies a group velocity in the y direction,

$$\langle n,X_0|v_y|n,X_0\rangle=-\frac{1}{m\omega_0}\frac{dE_n(X_0)}{dX_0}, \tag{6}$$

which is the expectation value of the velocity operator in the energy eigenstate ψ_{n,X_0}. It is the quantum equivalent to the classical drift velocity, i.e., the average velocity (in the y direction) along the corresponding classical orbit. The drift velocity in the x direction vanishes, since the orbits are bounded in the x direction.

Suitable units

For an economic comparison of classical and quantum aspects it is important to use suitable length and energy units, which are meaningful for both the quantum description and the classical limit. By doing so, we will see that the classical features depend on fewer scaled parameters than the quantum ones. To be specific but still rather general, we assume in the following periodic modulations of the form $B_m(x)=B_m^0\,b(Kx)$ and $U(x)=V_0\,u(Kx)$ for the magnetic and the electric modulation, respectively, where $b(\xi)$ and $u(\xi)$ are dimensionless periodic functions with period 2π and vanishing average values. Thus $B_m(x)$ and $U(x)$ have the same period $a=2\pi/K$, but may have different shapes and phases. In the numerical examples we will use for both $b(\xi)$ and $u(\xi)$ simple cosines, eventually with a phase shift.

The average magnetic field B_0 sets, with the magnetic length $l_0=\sqrt{\hbar/(m\omega_0)}$ and the cyclotron energy $\hbar\omega_0$, both a length and an energy scale, which are useful for quantum calculations, but have no meaning for the classical motion. For the discussion of commensurability effects, such as the Weiss oscillations, the cyclotron orbits must be compared with the period a of the modulation. Therefore a is a natural choice for the lengths unit. The choice of a suitable energy unit is motivated as follows.

Classically, B_0 determines only the cyclotron frequency ω_0, and one needs an independent length l to define an energy scale $V_{mag}=m\omega_0^2l^2/2$. Using l as the length unit, we may define dimensionless variables $\xi=x/l$ and $\xi_0=X_0/l$. The effective potential, Eq. (2), then can be written as $V(x;X_0)=V_{mag}\tilde{v}(\xi;\xi_0)$ with

$$\tilde{v}(\xi;\xi_0)=[\xi-\xi_0+s\,a(Kl\xi)/Kl]^2+w\,u(Kl\xi), \tag{7}$$

where $s=B_m^0/B_0$, $a(\zeta)=\int_0^\zeta d\zeta'\,b(\zeta')$, and $w=V_0/V_{mag}$. In the quantum description, the kinetic energy operator $-(\hbar^2/2m)d^2/dx^2=-E_l\,d^2/d\xi^2$, introduces an energy scale $E_l=\hbar^2/(2ml^2)$, which has no classical analog. Introducing the energy ratio $\alpha=E_l/V_{mag}$, we write the effective Schrödinger equation as

$$\left[-\alpha\frac{d^2}{d\xi^2}+\tilde{v}(\xi;\xi_0)-\tilde{\varepsilon}_n(\xi_0)\right]\tilde{\psi}_{n,\xi_0}(\xi)=0, \tag{8}$$

with $\tilde{\varepsilon}_n(\xi_0)=E_n(X_0)/V_{mag}$ and $\tilde{\psi}_{n,\xi_0}(\xi)=\sqrt{l}\,\psi_{n,X_0}(x)$.

If we would take $l=l_0$, we had $V_{mag}=E_l=\hbar\omega_0/2$ and thus simply $\alpha=1$. The effective potential Eq. (7) would then depend on the constant of motion ξ_0 and, in addition, on three dimensionless model parameters, s, w, and Kl_0. To specify an eigenstate or, in the classical description, a trajectory, one further needs an energy value $\tilde{\varepsilon}$ as a second constant of motion. A description that, for fixed constants of motion, needs *three* parameters to specify the effective potential and, furthermore, relies on l_0 and $\hbar\omega_0$, which have no meaning in classical mechanics, is rather clumsy and not acceptable.

Instead we take $l=1/K$ and, therefore, $V_{mag}=V_{cyc}$, where $V_{cyc}=m\omega_0^2/(2K^2)$ is the energy of a classical cyclotron orbit of radius $1/K$ in the homogeneous magnetic field B_0. Now the effective potential Eq. (7) depends only on the *two* dimensionless modulation strengths s and $w=V_0/V_{cyc}$, which both are well defined within the classical approach. Also the constants of motion, $\xi_0=KX_0$ and $\tilde{\varepsilon}=E/V_{cyc}=(KR_0)^2$, including the dimensionless version of Eq. (3),

$$\xi_0^{\pm}(\xi)=\xi+s\,a(\xi)\pm\sqrt{\tilde{\varepsilon}-w\,u(\xi)}, \tag{9}$$

remain meaningful in the classical limit. This choice of units will also be very useful for a systematic discussion of the quantum-mechanical energy spectra. Quantum mechanics enters the effective Schrödinger equation (8) only via the parameter $\alpha=(l_0K)^4$, which scales the kinetic energy. It determines the only true quantum aspect of the spectrum, namely the spacing of the energy levels $\tilde{\varepsilon}_n(\xi_0)$. We will see in Sec. III B that all the essential structural features of the energy spectrum, e.g., the complicated backfolded structure due to the coexistence of ''channeled'' and ''drifting'' states, are determined solely by the ''classical'' parameters s and w. The density of the quantized levels $\tilde{\varepsilon}_n(\xi_0)$, on the other hand, increases with increasing ratio a/l_0.

As a simple example one may consider the well known case of a weak electric or magnetic cosine modulation, which leads to modified Landau bands of oscillatory width.[2,4,18,19] The bandwidth assumes minima near the ''flat band'' energies $E_\lambda^{\pm}=m(\omega_0a)^2(\lambda\pm1/4)/8$, with ''+'' (''−'') for magnetic (electric) modulation and $\lambda=1,2,\ldots$. These flat band energies are distinct multiples of our energy unit V_{cyc}, and

occur at $\tilde{\varepsilon}_\lambda^{\pm} = \pi^2(\lambda \pm 1/4)$, independent of the special values of the model parameters B_0 and a. The level spacing, on the other hand, is of the order $\hbar\omega_0$ and depends in our units on $\hbar\omega_0/V_{\rm cyc} = 2l_0^2K^2 = 2\sqrt{\alpha}$.

III. MAGNETIC COSINE MODULATION

We first consider a pure magnetic modulation, $U(x) \equiv 0$, $B_m(x) = B_m^0\, b(Kx)$, so that the effective potential Eq. (7) becomes

$$V(\xi;\xi_0) = V_{\rm cyc}[\,\xi - \xi_0 + s\,a(\xi)]^2. \tag{10}$$

For $s=0$ one obtains the well known Landau levels and the Landau oscillator wave functions, $f_{nX_0}(x)$. We use the set f_{nX_0} as the basis of our Hilbert space in order to obtain numerical solutions for $s \neq 0$, by numerical diagonalization of $H(X_0)$. The electron effective mass is that of GaAs, $m = 0.067 m_0$. We further assume spin degeneracy. For the numerical parameters chosen here the size of the basis will vary between 150–300 Landau levels.

Before discussing the numerical results we summarize some properties of the effective potential and of Eq. (9), which now reduces to

$$\xi_0^{\pm}(\xi) = \xi + s\,a(\xi) \pm KR_0\,. \tag{11}$$

For a fixed ξ_0 the local extrema of the effective potential, given by $\partial V(\xi,\xi_0)/\partial\xi = 0$, are the points where the total magnetic field is zero, i.e., the roots of

$$1 + s\,b(\xi) = 0, \tag{12}$$

and the points where the effective potential is zero, i.e., the roots of

$$\xi - \xi_0 + s\,a(\xi) = 0. \tag{13}$$

An important aspect for the following discussion is that the roots of the first kind, Eq. (12), if existent, are independent of ξ_0, while those of the second kind, Eq. (13), do depend on ξ_0. We will see that orbits with ξ values near roots of the first kind are channeled, while those with ξ values near roots of the second kind are drifting orbits. The analytic dependence of the effective potential on the relevant position coordinate ξ is determined by the modulation strength s. Therefore the number of its possible zeroes, the classification of orbits, and the energy spectrum depend critically on the parameter s. To demonstrate this, we choose in the following examples $b(\xi) = \cos\xi$, and consequently $a(\xi) = \sin\xi$.

A. Weak modulation, $s \leqslant 1$

For $s<1$, the effective potential has exactly one minimum of the second kind for each value ξ_0, which is due to the confinement by the average magnetic field. The functions $\xi_0^{\pm}(\xi)$ in Eq. (11) have no extrema. For each value ξ_0 they determine exactly one orbit, which is a drifting cyclotron orbit. By this we mean a self-intersecting orbit consisting of loops along each of which the azimuth angle in velocity space, $\varphi = \arctan(v_y/v_x)$ increases by 2π. A typical example is illustrated in Fig. 1 for $s=0.5$, $\xi_0 = \pi/2$ (i.e., $X_0 = a/4$), and two energy values $E_{\rm F}$. Figure 1(a) shows the effective potential. For a given energy $E = E_{\rm F}$ (horizontal line) a classical orbit exists where $V(\xi;\xi_0) \leqslant E_{\rm F}$. Figure 1(b) shows the location of the turning points as the crossing points of the horizontal line $\xi_0 = \pi/2$ with the functions $\xi_0^{\pm}(\xi)$. The corresponding drifting orbit exists in the interval with $\xi_0^{-}(\xi) \leqslant \xi_0 \leqslant \xi_0^{+}(\xi)$. The orbits in real space are illustrated in Fig. 1(c). In Fig. 2 we plot the corresponding quantities for $s=0.5$ and $\xi_0 = \pi$ (i.e., $X_0 = a/2$). In this case the effective potential is symmetric with respect to the center coordinate X_0. As a consequence, the orbits are closed and their drift velocity in the y direction is zero.

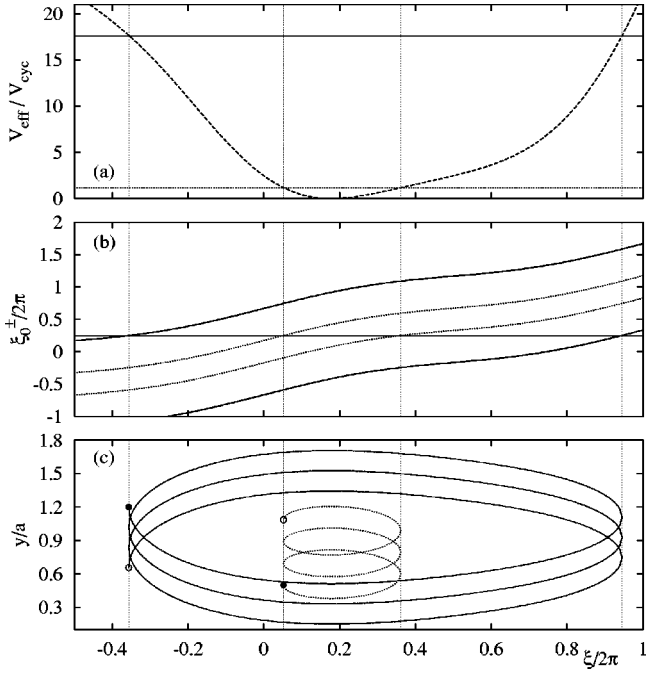

FIG. 1. (a) Effective potential $V(\xi;\xi_0)$ for magnetic cosine modulation with $s = B_m^0/B_0 = 0.5$ and $\xi_0/2\pi = 1/4$. For a given energy $E_{\rm F}/V_{\rm cyc} = (KR_0)^2$ (horizontal lines) classical orbits exist where $V(\xi;\xi_0) \leqslant E_{\rm F}$. Solid line, $E_{\rm F} = 17.6 V_{\rm cyc}$; dotted line, $E_{\rm F} = 1.18 V_{\rm cyc}$. (b) Locations of turning points $\xi_0^{\pm}(\xi)$ for the $E_{\rm F}$ values indicated in (a), same coding. Orbits with energy $E_{\rm F}$ and ξ_0 exist in an interval with $\xi_0^{-}(\xi) \leqslant \xi_0 \leqslant \xi_0^{+}(\xi)$. (c) Corresponding orbits in xy space, three cycles are shown each, the sense of motion is from filled to open dot.

For small energies, $E_{\rm F}/V_{\rm cyc} = (KR_0)^2 < \pi^2$ (i.e., $2R_0 < a$), the extents of the orbits in the x direction are smaller than a modulation period and essentially determined by the local values of the total magnetic field. At high energies, $E_{\rm F}/V_{\rm cyc} \gg 1$, the orbits extend over several periods of the modulation and the extent of an orbit, i.e., the width of the effective potential valley at the corresponding energy, is determined by the cyclotron radius in the average magnetic field ($x_r - x_l \approx 2R_0$).

In Fig. 3(a) we display the first 50 energy bands $E_{n\xi_0}$ calculated from the (first 150) original, degenerated Landau levels, for $s=0.5$. The level spacing of the lowest-energy bands is seen to follow the local value of the total magnetic field, Fig. 3(b). This is expected from the local approximation $E_{n\xi_0} \approx (n+1/2)\hbar eB(\xi_0)/m$, which is valid if the extent of the wave functions $\psi_{n,X_0}(x)$ is smaller than the modulation period. With our energy unit $V_{\rm cyc}$ the apparent level

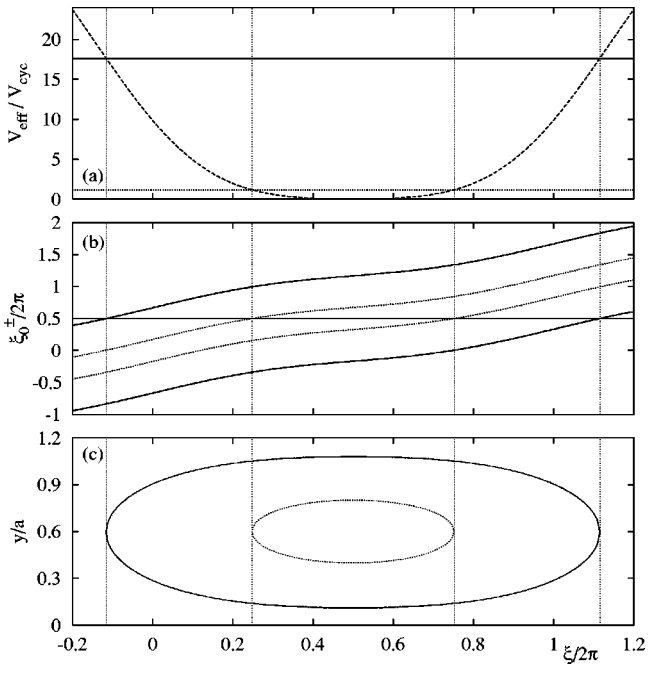

FIG. 2. As Fig. 1, but $\xi_0/2\pi=1/2$. The effective potential is symmetric and therefore the guiding center of these drifting orbits does not drift in (c).

spacing of energies which are independent of the period a becomes proportional to $\sqrt{\alpha}$. For example, if the local approximation $E_{n\xi_0}\approx(n+1/2)\hbar\omega(\xi_0)$ holds for $E_{n\xi_0}<4V_{\rm cyc}$, as in Fig. 3(a), this implies that it holds for $n+1/2<4V_{\rm cyc}/[\hbar\omega(\xi_0)]=2[\omega_0/\omega(\xi_0)]/\sqrt{\alpha}$. Thus, the number of bands which are well described by the local approximation increases quadratically with increasing modulation period a.

The local approximation fails at higher energies when the width of the wave functions becomes larger than the period of the modulation, and the structure of the energy spectrum changes. Indeed it is well known from the limit of very weak magnetic modulation, $s\ll1$, that in contrast to this local approximation the bands become flat at the energies $E_\lambda/V_{\rm cyc}=\pi^2(\lambda+1/4)$, for $\lambda=1,2,\ldots$.[18,19,6] These flat band conditions are the quantum equivalents to the classical commensurability conditions leading to the Weiss oscillations in magnetotransport, and do not change their positions in a plot like Fig. 3(a), even if we change the modulation period. A larger modulation period a just leads to a higher density of the energy bands.

In Fig. 3(c) we plot for $\xi_0=\pi/2$ the effective potential and the square of the energy eigenfunctions for the energy values considered in Fig. 1. Width and location of the wave functions in the effective potential is in close agreement with that of the corresponding classical orbits. In Fig. 3(d) we plot the corresponding quantities for the symmetric situation $\xi_0=\pi$, to be compared with Fig. 2. These wave functions belong to (relative) extrema of the energy bands, and thus have zero group velocity, in agreement with the zero drift velocity of the corresponding classical orbits. The wave functions in Fig. 3(c) belong to finite energy dispersion and describe motion in the positive ($n=3$) and the negative ($n=43$) y direction, respectively, in agreement with the correponding classical orbits in Fig. 1. For large quantum numbers n and weak

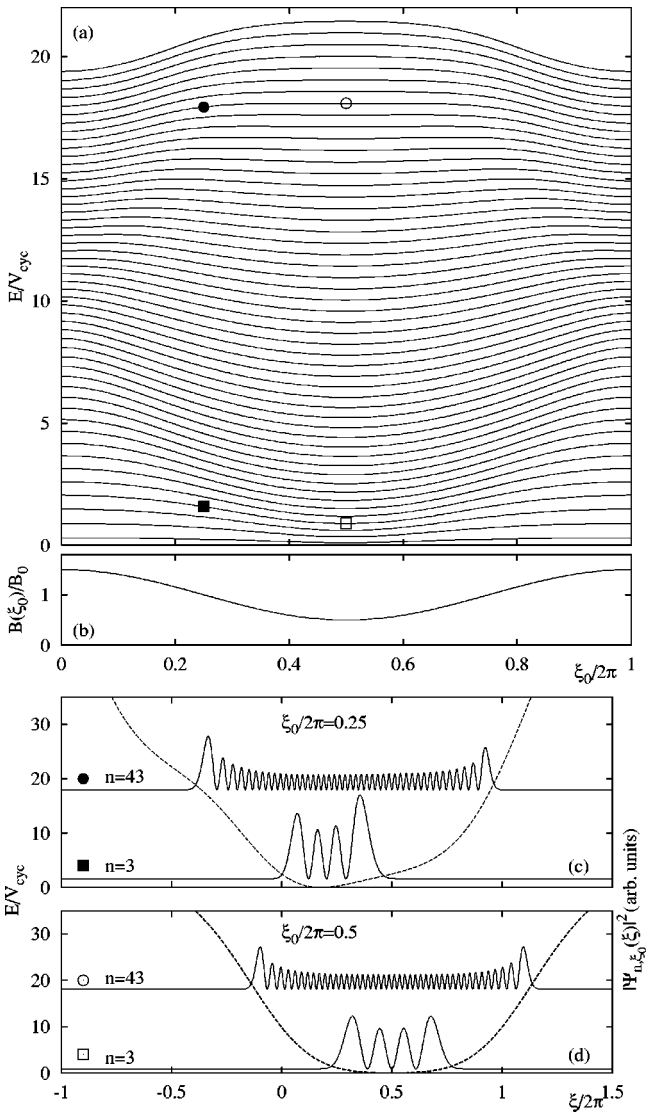

FIG. 3. (a) Landau bands for $s=0.5$. $B_0=0.2$ T and $a=800$ nm, so that $V_{\rm cyc}=0.85$ meV and $\alpha=0.041$ and (b) total magnetic field $B(\xi_0)$. The marked points on Landau bands 43 and 3 are the states for which the wave functions are shown in (c) and (d) in arbitrary units together with the corresponding effective potentials (dashed line). The wave functions are plotted with an offset, indicating the energy of the state. The states of (c) and (d) are to be compared with the classical orbits in Figs. 2 and 1, respectively.

modulation the group velocities can be shown to reduce quantitatively to the drift velocities of the corresponding classical orbits.

In Fig. 4 we consider the ''critical'' situation $s=1$. The derivatives $\xi_0^{\pm\prime}(\xi_{ex})=0$ and $\xi_0^{\pm\prime\prime}(\xi_{ex})=0$ vanish for $\xi_{ex}=(2p+1)\pi$ (p integer), i.e., for the positions where the magnetic field vanishes, Eq. (12). For all values of ξ_0 the effective potential (7) becomes flat at these points ξ_{ex} [see Fig. 4(c)]. The classical situation is as for $s<1$ with the exception that for $\xi_0=\xi_{ex}\pm KR_0$ there are critical orbits which asymptotically approach straight lines parallel to the y axis on their left (for $+$) or their right (for $-$) side, where $B(x)=0$. The dashed lines plotted over the energy spectrum of Fig. 4(a) show the evolution of the flat regions of the effective potential with ξ_0, i.e., the parabolas resulting from

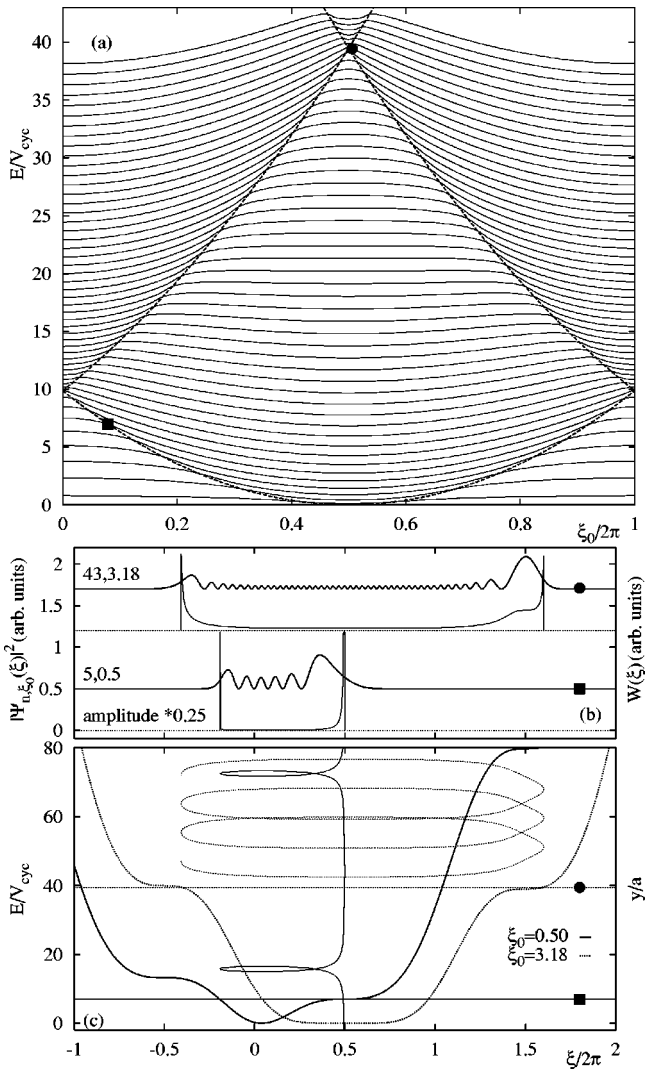

FIG. 4. (a) Energy spectrum for $s=1$. $B_0=0.1$ T and $a=800$ nm, so that $V_{\rm cyc}=0.21$ meV and $\alpha=0.17$. The dashed lines show $V(\xi_0,(2p+1)\pi)$ with $|p|\leqslant 1$. (b) Quantum-mechanical (thick lines) and corresponding classical (thin lines) probability densities for two states. The chosen states are marked with dots in (a). (c) Effective potentials and classical orbits for $E_{\rm F}=7V_{\rm cyc}, \xi_0=0.5$ (solid lines) and $E_{\rm F}=39.6V_{\rm cyc}, \xi_0=3.18$ (dotted lines). The horizontal lines indicate the Fermi energy.

$V(\xi_{ex};\xi_0)$ with $p=0$ and $p=\pm 1$. In the first Brillouin zone these lines are seen as the backfolding of the lowest parabola centered on ξ_{ex} with $p=0$, and they are an indication of a kind of a free-electron motion along the lines where the magnetic field is zero. Close to these parabolas the energy bands have large dispersion near inflexion points, and the energy separation between adjacent bands is minimum. Similar features have been obtained in the energy spectra for single magnetic wells by Peeters and Matulis.[20] In other words, such states experience a weak effective magnetic field, due to the constant effective potential over a substantial spatial region. The wave functions corresponding to states with large energy dispersion have large amplitudes at the positions of flat effective potential (vanishing total magnetic field). This is demonstrated for two selected states [$(n=43,\ \xi_0=3.18)$ and $(n=5,\ \xi_0=0.50)$] in Fig. 4(b), together with the probability distributions of the corresponding classical orbits. The effective potentials together with the corresponding classical orbits are plotted in Fig. 4(c). The trajectory corresponding to the state $(n=5,\ \xi_0=0.50)$ is close to a critical orbit with a critical right turning point. This leads to an enhanced probability density near that point, which is also reflected in the quantum mechanical probability density. We will see that for slightly stronger modulation a type of nearly free motion occurs with energies close to the parabolas $V(\xi_{ex};\xi_0)$ in the energy spectrum.

B. Strong modulation, $s>1$

For $s>1$, $\xi_0^{\pm\,\prime}(\xi)=0$ at $a(\xi)\equiv\cos\xi=-1/s$, and $\xi_0^{\pm}(\xi)$ has extrema at the following positions:

$$\text{minima:}\quad \xi_{min}^{(p)}=(2p+1)\pi+\delta,$$

$$\text{maxima:}\quad \xi_{max}^{(p)}=(2p+1)\pi-\delta, \tag{14}$$

where p is an integer and $\delta=\arctan\sqrt{s^2-1}$. The values at these extrema are

$$\xi_0^{\pm}(\xi_{min}^{(p)})=(2p+1)\pi-g(s)\pm KR_0,$$

$$\xi_0^{\pm}(\xi_{max}^{(p)})=(2p+1)\pi+g(s)\pm KR_0, \tag{15}$$

where

$$g(s)=\sqrt{s^2-1}-\arctan\sqrt{s^2-1}>0. \tag{16}$$

The effective potential $V(\xi;\xi_0)$ has extrema of the first kind, Eq. (12), at the same positions. The extrema with values $V(\xi_{min}^{(p)};\xi_0)=V_{\rm cyc}[(2p+1)\pi-g(s)-\xi_0]^2$ are minima if $(2p+1)\pi>\xi_0$, and maxima otherwise, and those with values $V(\xi_{max}^{(p)};\xi_0)=V_{\rm cyc}[(2p+1)\pi+g(s)-\xi_0]^2$ are maxima if $(2p+1)\pi>\xi_0$, and minima otherwise.

1. Classical approach

The number of zeroes of $\xi_0^{\pm}(\xi)-\xi_0$ depends on both s and ξ_0. If $g(s)<\pi$, $\xi_0^{\pm}(\xi)-\xi_0$ has at most three zeroes. If $\xi_0=\xi_0^{\pm}(\hat{\xi})$ for any $\hat{\xi}$ satisfying $\xi_{max}^{(p)}<\hat{\xi}<\xi_{min}^{(p)}$, i.e., if $(2p+1)\pi-g(s)<\xi_0\mp KR_0<(2p+1)\pi+g(s)$, $\xi_0^{\pm}(\xi)-\xi_0$ has three zeroes. The same argument holds for Eq. (13), i.e., the effective potential has three zeroes. For $(2p-1)\pi+g(s)<\xi_0\mp KR_0<(2p+1)\pi-g(s)$, on the other hand, there exists only a single zero.

In Fig. 5 we show, for $s=2$ [i.e., $g(s)=0.685$], an example where the effective potential has a single zero near $\xi/2\pi=0.1$, so that for sufficiently low energy only a single drifting orbit exists. The number and the type of the possible orbits depend on the energy. At the highest energy shown in Fig. 5(a) two orbits exist [solid lines in Fig. 5(d)]. There is a drifting cyclotron orbit extending over more than two periods of the modulation, with the left turning point on $\xi_0^{+}(\xi)$ [uppermost curve in Fig. 5(c)] near $\xi/2\pi=-1.1$, and the right turning point on $\xi_0^{-}(\xi)$ [bottom curve in Fig. 5(c)] near $\xi/2\pi=1.3$. Near the relative minimum of $\xi_0^{-}(\xi)$ close to $\xi/2\pi=1.7$, which corresponds to a relative minimum of the effective potential [thick dashed line in Fig. 5(a)], there exists a ''channeled orbit'' moving in the positive y direction. We define channeled orbits as trajectories which have both turning points either on $\xi_0^{+}(\xi)$ or on $\xi_0^{-}(\xi)$, in contrast to the

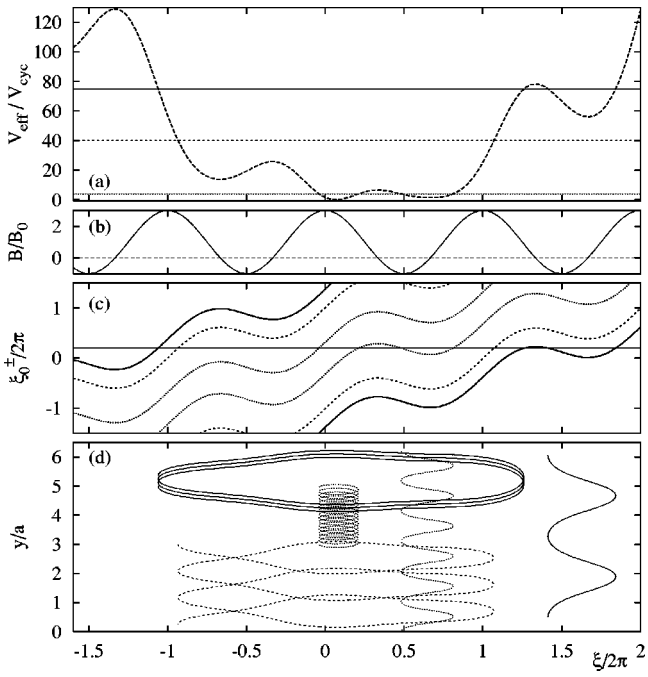

FIG. 5. (a) Effective potential $V(\xi;\xi_0)$ for magnetic cosine modulation with $s=B_m^0/B_0=2$, and $\xi_0/2\pi=0.2$. For given energy E_F (horizontal lines) classical orbits exist where $V(\xi;\xi_0)\leqslant E_F$. (b) Total magnetic field. (c) Locations of turning points $\xi_0^{\pm}(\xi)$ for the E_F values indicated in (a). The outermost pair of lines belongs to the largest E_F value; the innermost pair belongs to the smallest E_F value. The constant of motion ξ_0 appears as a horizontal line in this plot ($\xi_0/2\pi=0.2$ is indicated). Orbits with fixed energy [i.e., fixed curves $\xi_0^{\pm}(\xi)$] and this value of ξ_0 exists in intervals with $\xi_0^-(\xi)\leqslant\xi_0\leqslant\xi_0^+(\xi)$. Orbits, plotted in (d), with one turning point on $\xi_0^-(\xi)$ and the other on $\xi_0^+(\xi)$ are drifting orbits, the others are channeled orbits (see text).

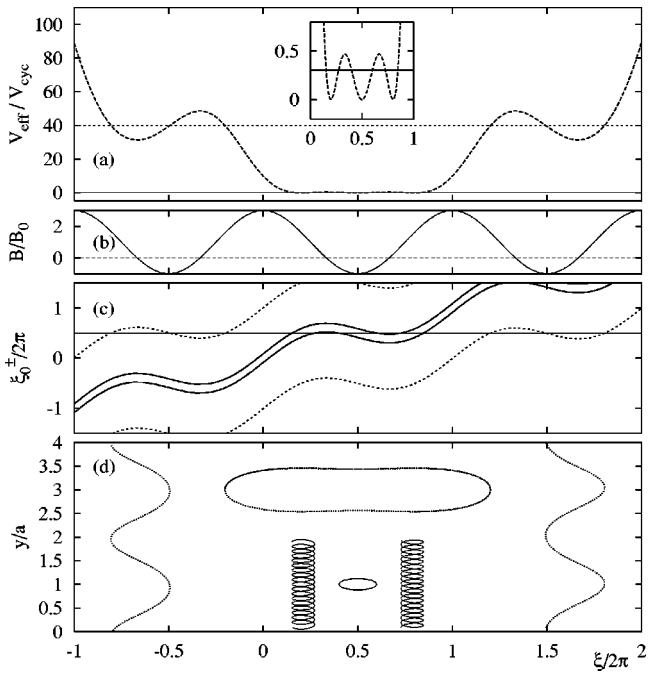

FIG. 6. As in Fig. 5 but for $s=2$, and $\xi_0/2\pi=0.5$. Horizontal lines in (a) are for $E_F/V_{cyc}=40$ and $E_F/V_{cyc}=0.3$. The inset shows $V(\xi;\xi_0)$ enlarged between $\xi=0$ and $\xi=2\pi$, where it has three zeroes. (c) For both indicated energies there exist three orbits, one drifting and two channeled orbits for $E_F/V_{cyc}=40$, and three drifting orbits for $E_F/V_{cyc}=0.3$, plotted in (d). Since the effective potential is symmetric, there is no guiding center drift for the central drifting orbits.

drifting orbits with one turning point on $\xi_0^+(\xi)$ and the other on $\xi_0^-(\xi)$. In contrast to the self-intersecting drifting orbits, the channeled orbits are always confined to less than a single modulation period, and they move without self-intersections in a relatively narrow interval of angles around the positive or the negative y direction [see Fig. 5(d)]. Note that the curvature of the trajectories changes sign at the positions where the total magnetic field vanishes, see Fig. 5(b).

If we lower the energy to $E/V_{cyc}=40$, we arrive in Fig. 5 at a situation where only a single drifting orbit exists (dashed lines). In general, the extent in the ξ direction of the drifting orbits decreases with decreasing energy. At the lowest energy indicated in Fig. 5 [lowest dotted line in (a) and innermost lines in (c)], we have again a drifting orbit near $\xi/2\pi=0.1$ and a channeled orbit around $\xi/2\pi=0.6$. At this low energy, the extent of the drifting orbit is considerably smaller than the modulation period.

In Fig. 6 we show, for the same modulation strength, $s=2$, a situation, $\xi_0=\pi$, where the effective potential has three zeroes, as is emphasized in the inset of Fig. 6(a). These zeroes are separated by two shallow maxima. If a (positive) E value below these maxima is chosen, one finds three narrow drifting cyclotron orbits located around the zeroes of the effective potential (solid lines). For higher energies one may find either one drifting and two channeled orbits (dotted lines) or a single drifting orbit (e.g., for $0.5<E/V_{cyc}<30$, not indicated in the figure). Actually the ''drifting'' orbits located around $\xi=\pi$ have zero drift velocity due to symmetry reasons.

In summary, for $0<g(s)<\pi$ we find for given values of the constants of motion, ξ_0 and E, at least one and at most three orbits. For larger values of $s=B_m^0/B_0$, more orbits may exist for a given pair of ξ_0 and E values. A careful analysis of the extrema of the functions $\xi_0^{\pm}(\xi)$ shows, e.g., that for $\pi<g(s)<2\pi$ between three and five orbits belong to the same pair of ξ_0 and E. We will come back to this case below.

Apparently the plots of the effective potential $V(\xi;\xi_0)$ are very useful to see which orbits are possible for a fixed value of the center coordinate ξ_0 and different energies. Channeled orbits exist in side valleys near relative minima of $V(\xi;\xi_0)$. If, on the other hand, the energy of the motion is given, the plots of the locations of turning points $\xi_0^{\pm}(\xi)$ is very useful to classify the possible orbits for different values of ξ_0. Channeled orbits exist near relative minima of $\xi_0^-(\xi)$ and relative maxima of $\xi_0^+(\xi)$.

2. Quantum calculation

The energy spectra become more complicated in the case $s>1$, Figs. 7 and 8. Regions of different character can be distinguished in these spectra. Areas, where the energy bands are nearly parallel lines with low dispersion (region I) alternate with regions, where steep bands with large dispersion seem to cross bands with weak dispersion (region II). In fact the energy bands never cross each other and the apparent intersections are anticrossing points with exponentially small gaps.

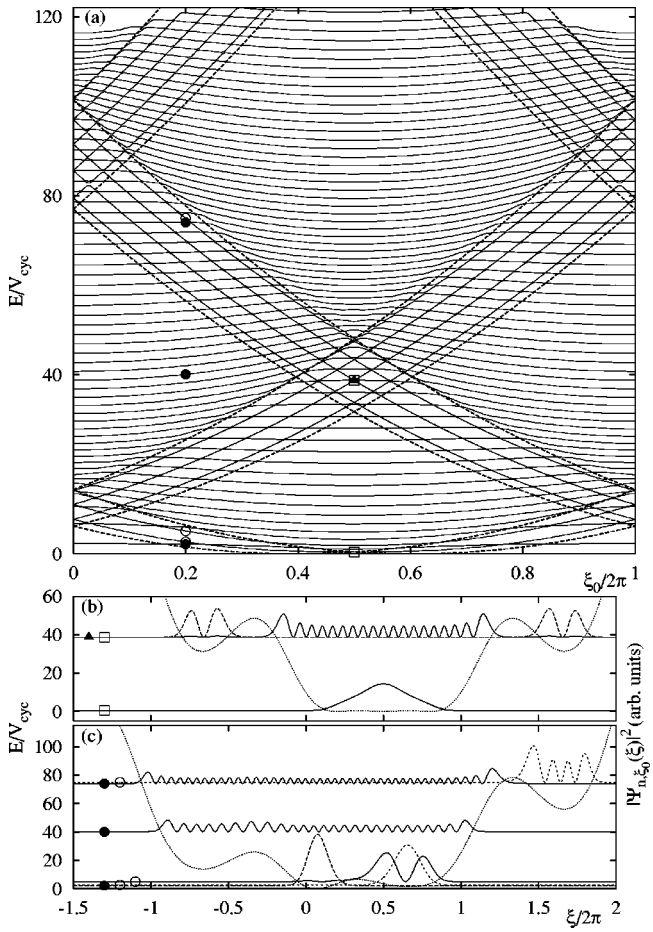

FIG. 7. (a) Energy spectrum (first 75 bands) for $s=2$. $B_0=0.05$ T and $a=800$ nm, so that $V_{\mathrm{cyc}}=0.053$ meV and $\alpha=0.67$. Effective potential and specific states (b) ($n=0,20,22$) for $\xi_0/2\pi=0.5$ and (c) ($n=0,1,2,25,44,45$) for $\xi_0/2\pi=0.2$.

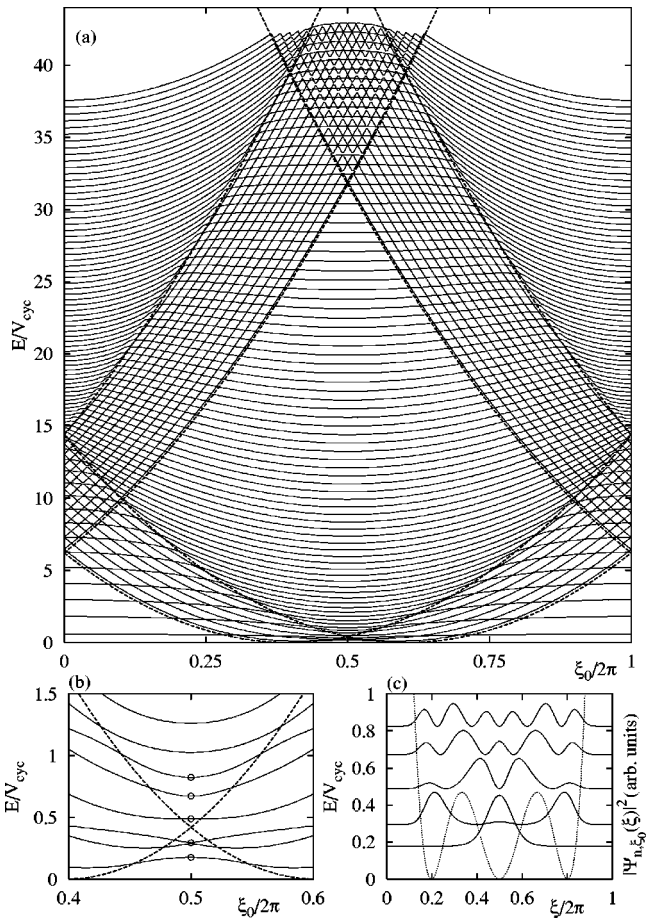

FIG. 8. (a) Energy spectrum (first 100 bands) for $s=2$. $B_0=0.2$ T and $a=800$ nm, so that $V_{\mathrm{cyc}}=0.851$ meV and $\alpha=0.041$. (c) Effective potential and specific states ($n=0,2,3,4,5$), marked in extract of spectrum (b), for $\xi_0/2\pi=0.5$.

The boundaries of these regions are given by classical values only. If the energy is scaled by the classical cyclotron energy V_{cyc}, for fixed modulation strength s the regions II are surrounded by the parabolas $E=V(\xi_{\min}^{(p)};\xi_0)$ and $E=V(\xi_{\max}^{(p)};\xi_0)$ which, for $|p|\leqslant 2$, are indicated by dashed lines in the spectra. For any fixed ξ_0 such a pair of parabolas gives the minimum and the maximum value of a certain side valley of the effective potential $V(\xi;\xi_0)$ [extrema of the first kind, see Eq. (12)]. The energy interval in between these values indicates the depth of that valley, i.e., an energy range in which classically channeled orbits exist, in addition to the drifting orbits.

In Fig. 7(b) the effective potential is plotted for the symmetric case $\xi_0=\pi$ (dotted line), corresponding to the classical situation described in Fig. 6. Also shown are the states for $n=0$ (lower solid line) and for $n=20$ (upper solid line) and $n=22$ (upper dashed line). Apparently, state $n=20$ corresponds to a classical drifting orbit, whereas $n=22$ is the symmetric superposition of two states corresponding to channeled orbits in the side valleys. The latter has practically the same energy as the corresponding antisymmetric superposition ($n=21$), which is not shown. On the scale of Fig. 7(a), all states $n=20$, 21, and 22 seem to have the same energy, $E/V_{\mathrm{cyc}}\approx 38$. The states $n=21$ and 22 are hybridizations of states belonging to the branches with high-energy dispersion and the opposite sign of the group velocity

$$\langle v_y\rangle=-\frac{K}{m\omega_0}\frac{dE_{n\xi_0}}{d\xi_0}. \tag{17}$$

Figure 7(c) shows the effective potential for the asymmetric case $\xi_0/2\pi=0.2$, corresponding to the classical situation described in Fig. 5. Here we show six states, the ground state $n=0$ located near the zero of the effective potential, the two ''channeled'' states ''bound'' in the potential valley around $\xi/2\pi=0.6$, the extended drifting state $n=25$ near $E=40V_{\mathrm{cyc}}$, the extended state $n=44$, and the localized channeled state $n=45$. The energies of all these states are indicated in Fig. 7(a). The states which extend over more than a period of the modulation belong to weakly dispersive energy bands and correspond to the classical drifting orbits. The states belonging to the energy branches with strong dispersion have large amplitudes in side valleys of the effective potential and vanish practically outside these valleys. They correspond to classical channeled orbits. The apparent number of nodes of the large-amplitude parts of these channeled states increases with energy as if they were truly bound states in these narrow valleys. Note, however, that the wave functions of channeled states still have n nodes, but the corresponding oscillations are not observable at the scale of the

figure. Outside the valleys, the maxima in between the nodes are a few orders of magnitude smaller than the main peaks inside the valleys.

The number of quantized states within a given valley of the effective potential depends on the average magnetic field and the period of the magnetic modulation, even if the parameters V_{cyc} and s are fixed. In Fig. 7 the period a, or the field B_0, is too small to have states quantized in the low-energy triple minimum of the effective potential for the symmetric case of Fig. 7(b) (see also Fig. 6). To investigate this situation, we show in Fig. 8(a) a denser spectrum for the same modulations strength $s=2$. In Fig. 8(b) the spectrum near $\xi_0=\pi$ is enlarged. Five energy values are indicated, and in Fig. 8(c) the corresponding (squares of the) wave functions are plotted for the states $n=0$, 2, 3, 4, and 5, together with the effective potential. The antisymmetric state $n=1$, which is nearly degenerate with $n=2$, is not shown. This demonstrates that all the classical features have their quantum analog, provided the model parameters (here α) are suitably chosen.

For the magnetic cosine modulation, the depth of the valleys of the effective potential,

$$|V(\xi_{\max}^{(p)};\xi_0)-V(\xi_{\min}^{(p)};\xi_0)|/V_{cyc}=4g(s)|(2p+1)\pi-\xi_0|, \tag{18}$$

increases with the energy (i.e., with $|p|$ for fixed ξ_0), and thus more and more channeled states appear at higher energies. For sufficiently high energies the strips with channeled states in the energy spectra may thus extend over the whole Brillouin zone. This will also happen for sufficiently large s. The energy dispersion of the channeled states depends strongly, nearly quadratically, on ξ_0 according to Eq. (10), which expresses the nearly free motion of the electrons on channeled orbits in the y direction.

For $s>1$ and $g(s)<\pi$, the area of the regions II of the spectrum increases with increasing s, and the area of the regions I shrinks accordingly. For $g(s)=\pi$, one has $V(\xi_{\min}^{(p)};\xi_0)=V(\xi_{\max}^{(p-1)};\xi_0)$ and the corresponding parabolas coincide, leaving no room for regions I. If the modulation is so large that $g(s)\geqslant\pi$, drifting and channeled states coexist everywhere in the spectrum. In Fig. 9 we have chosen $s=5$, corresponding to $g(s)=3.53$. Close to the edges of the Brillouin zone, e.g., for $\xi_0/2\pi=0.016$, Fig. 9(c), we can identify channeled, e.g., $n=22$ and 16, and drifting states, e.g., $n=19$. But now these drifting states are relatively narrow, confined in local minima of the effective potential and not in the wide potential-well centered around ξ_0, which is given by the confinement due to the average magnetic field. This case is already known from the discussion of Fig. 6. The local minimum of the effective potential at $\xi=0$ is a minimum of the second kind, with vanishing potential. Consequently, these drifting states are similar to weakly perturbed Landau levels with energy gaps $\hbar eB(\xi_0)/m$, as can be observed by a careful look at Fig. 9(a). In the center of the Brillouin zone, say for $\xi_0/2\pi=0.493$, Fig. 9(d), the effective potential has three zeroes of the second kind [see Eq. (13)] near $\xi=\xi_0$. We, therefore, can find similar narrow drifting states, such as $n=5$ and 6, but also wide drifting states at higher energies, like $n=17$ and channeled states in local minima of the first kind, such as $n=7$. As in the classical

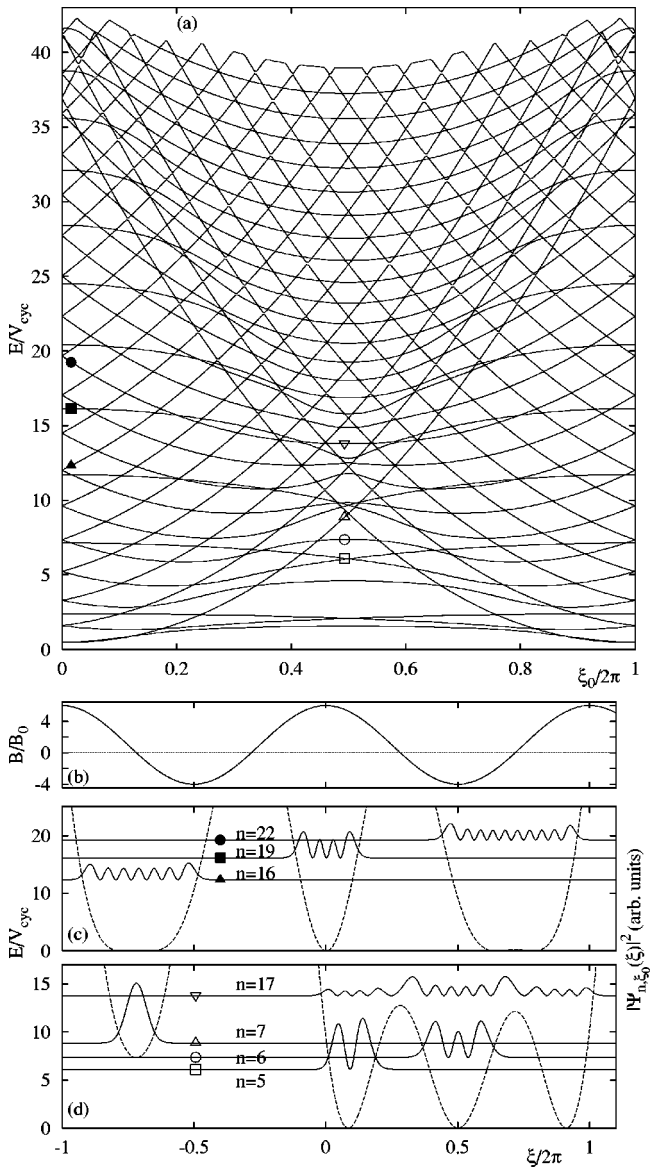

FIG. 9. (a) Energy spectrum for $s=5$. $B_0=0.1$ T and $a=800$ nm, so that $V_{cyc}=0.213$ meV and $\alpha=0.16$. (b) Total magnetic field. (c) Effective potential and specific states for $\xi_0/2\pi=0.016$. Typical channeled states $n=16$ and 22 and narrow drifting states, $n=19$. (d) Effective potential and specific states for $\xi_0/2\pi=0.493$. Wide drifting state, $n=17$, narrow drifting states, $n=5$ and 6, and a channeled state, $n=7$.

picture, the velocity of these narrow drifting states is in general lower than that of the channeled states.

IV. MIXED HARMONIC MODULATIONS

For sufficiently strong mixed electric and magnetic modulations one expects a similar situation as for the strong magnetic modulation, with a coexistence of channeled and drifting orbits, and their quantum analogs. In the presence of an electric modulation, we have no explicit analytic expressions for the minima of the effective potential, Eq. (7), not even for simply harmonic modulations. Nevertheless, a qualitative understanding of the classical and the corresponding quantum-mechanical motion is possible. For a given constant of motion ξ_0 the effective potential has side valleys with

possible channeled orbits, if $\partial V(\xi;\xi_0)/\partial\xi=0$ has more than one solution ξ. This is the case if the function

$$\xi_0(\xi)=\xi+s\,a(\xi)-\frac{w}{2}\,\frac{u'(\xi)}{1+s\,b(\xi)}, \tag{19}$$

with $w=V_0/V_{\rm cyc}$, assumes the value $\xi_0(\xi)=\xi_0$ at more than one ξ value. At such ξ values the effective potential has extrema with the values

$$V(\xi;\xi_0(\xi))/V_{\rm cyc}=w\,u(\xi)+\left[\frac{w}{2}\,\frac{u'(\xi)}{1+s\,b(\xi)}\right]^2. \tag{20}$$

To be specific, we choose for the following $b(\xi)=\cos\xi$, $a(\xi)=\sin\xi$ and $u(\xi)=\cos(\xi+\varphi_s)$.

Apparently, Eqs. (19) and (20) provide a parametric representation of the possible relative extrema of the effective potential in the energy-versus-ξ_0 diagram, similar to the dashed lines in Figs. 7 and 8 which define the regions II where channeled states coexist with drifting ones. Due to the symmetries $\xi_0(\xi+2\pi)=\xi_0(\xi)+2\pi$ and $V(\xi+2\pi;\xi_0(\xi+2\pi))=V(\xi;\xi_0(\xi))$, it is sufficient to consider only one period $0\leqslant\xi\leqslant 2\pi$ of the parameter ξ, provided the $\xi_0(\xi)$ values are backfolded into the first Brillouin zone.

For strong magnetic modulation ($s>1$) the denominators in Eqs. (19) and (20) lead to poles. Then the regions of type II extend to arbitrary high energies, similar to the case of pure magnetic modulation. A qualitatively different behavior is obtained for weak magnetic, but arbitrarily strong electric modulation, since then the denominators of Eqs. (19) and (20) remain positive (for $s<1$). Consequently, for given values of w, s, and φ_s the possible values of $V(\xi;\xi_0(\xi))$, Eq. (20), are bound and channeled orbits can exist only below a certain energy.

A. Pure electric modulation

As a particularly simple example we consider a pure electric cosine modulation, $s=0$, $\varphi_s=0$. For weak modulation ($w<2$) the function $\xi_0(\xi)$ of Eq. (19) has a unique inverse, i.e., the effective potential $V(\xi;\xi_0)$ has for all values of ξ_0 only a single extremum, namely the absolute minimum, and no channeled states should be expected. The energy spectra for this weak-modulation limit are well known[2,3,13] and will not be reproduced here. Apart from a phase shift, they look similar to Fig. 3(a) but with flat bands near $E/V_{\rm cyc}=\pi^2(\lambda-1/4)$, for $\lambda=1, 2, \ldots$.

The corresponding classical trajectories at sufficiently high energies are drifting cyclotron orbits. At very low energies, $E<V_0=wV_{\rm cyc}$, a peculiarity occurs, since then the classical trajectories are captured within a single valley of the electric potential, with turning points given by Eq. (9) in the interval $\xi_c\leqslant\xi\leqslant 2\pi-\xi_c$ (modulo 2π) with $\xi_c=\arccos(E/V_0)>0$. For ξ_0 values in the interval $\xi_c<\xi_0<2\pi-\xi_c$ these trajectories are self-intersecting drifting orbits, whereas for $\xi_0<\xi_c$ and $\xi_0>2\pi-\xi_c$ there exist channeled orbits with $v_y>0$ and $v_y<0$, respectively. The orbit with $\xi_0=\xi_c$ approaches the left turning point at $\xi=\xi_c$ with a tangent parallel to the x axis, and that with $\xi_0=2\pi-\xi_c$ does the same at the right turning point $\xi=2\pi-\xi_c$. This peculiar low-energy behavior is, of course, not restricted to the weak modulation limit, but occurs always when the trajectories are captured in a minimum of the electric potential, i.e., for $E<V_0$. It is demonstrated in Fig. 10(b), and will not be discussed further.

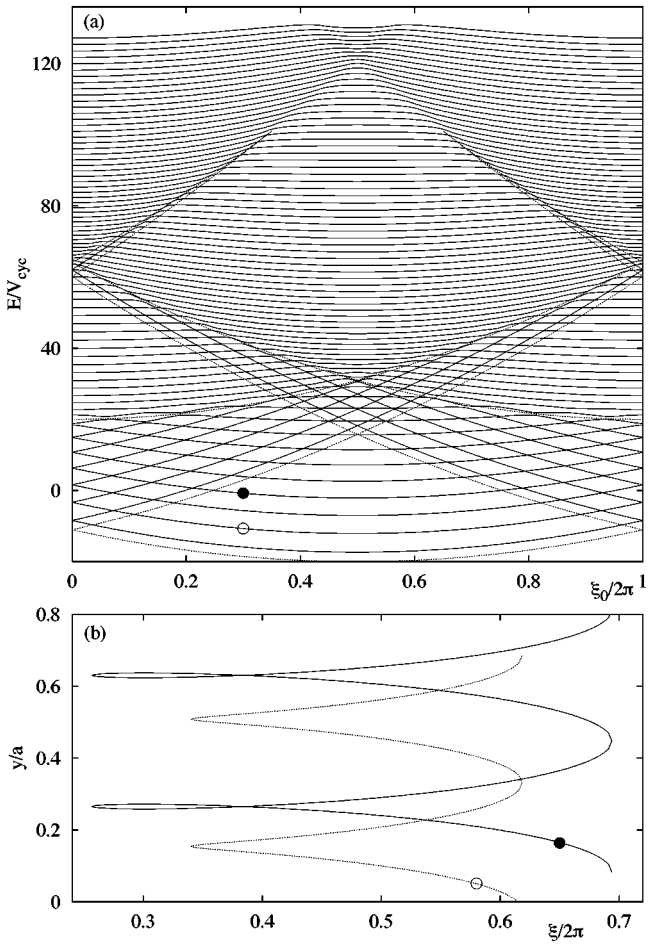

FIG. 10. Pure electric modulation of strength $w=20$. (a) Energy spectrum (first 80 bands) for $B_0=0.05$ T and $a=800$ nm, so that $V_{\rm cyc}=0.053$ meV and $\alpha=0.67$. (b) Drifting orbit (solid line) and channeled orbit (dotted line) for $\xi_0/2\pi=0.3$. The energies [see marked states in (a)] are chosen in such a way that $\xi_c<\xi_0$ for the drifting and $\xi_c>\xi_0$ for the channeled orbit, see text.

If the electric modulation is strong enough, $w>2$, the function $\xi_0(\xi)=\xi-(w/2)\sin\xi$, Eq. (19), has extrema at $\xi_+=\arccos(2/w)>0$ and $\xi_-=-\xi_+$ (modulo 2π) with values $\xi_0(\xi_\pm)=\mp g(w/2)$, where $g(s)$ is defined by Eq. (16). Then, for $|\xi_0|\leqslant g(w/2)$ the equation $\xi_0(\xi)=\xi_0$ has three solutions ξ in the interval $|\xi|<\pi$, which are local extrema of the effective potential with values

$$V(\xi;\xi_0(\xi))/V_{\rm cyc}=1+(w/2)^2-[1-(w/2)\cos\xi]^2. \tag{21}$$

In order to find in the energy spectra the regions II corresponding to side valleys of the effective potential, one may proceed as follows. One plots in the extended zone scheme $V(\xi;\xi_0(\xi))$ versus $\xi_0(\xi)$, starting at $\xi=-\pi$, where $\xi_0(\xi)=-\pi$ and $V(\xi;\xi_0(\xi))=-V_0$. With increasing ξ, also $\xi_0(\xi)$ and $V(\xi;\xi_0(\xi))$ increase and reach at $\xi=\xi_-$ their maximum values $g(w/2)$ and $V_{\rm cyc}(1+w^2/4)$, respectively. As ξ increases from $\xi=\xi_-$ to $\xi=0$, $\xi_0(\xi)$ and $V(\xi;\xi_0(\xi))$ decrease towards the values 0 and V_0, respectively. Increasing ξ from 0 to π leads to the mirror image of the described trace with

respect to $\xi_0=0$: $\xi_0(\xi)=-\xi_0(-\xi)$ and $V(\xi;\xi_0(\xi))=V(-\xi;\xi_0(-\xi))$. Finally these four line segments have to be folded back into the ''first'' Brillouin zone $0\leqslant\xi_0\leqslant 2\pi$ to obtain the absolute minimum of the effective potential as a function of ξ_0 and the boundaries of the regions II. In contrast to the strong magnetic modulation, these regions become narrower with increasing energy and end at $\xi_0=\pm g(w/2)$ (modulo 2π) with energy $E/V_{\rm cyc}=1+w^2/4$. For $g(w/2)>\pi$ the backfolding leads to an overlap of different branches of the region II that is the coexistence of back and forth running channeled states with drifting states in the same area of the E-ξ_0 diagram. Figure 10 shows for a typical example the quantum-mechanical energy spectrum together with the boundaries of region II obtained in this manner. The ''very complicated'' energy spectrum obtained recently by Shi and Szeto[13] for strong electric modulation is thus explained by the coexistence of channeled and drifting states.

In previous work[10,11] it was pointed out that, for given modulation period a and strength V_0 and given energy $E=E_{\rm F}$, channeled orbits can exist only if the magnetic field B_0 is smaller than a critical field $B_{\rm crit}$. Solving $E_{\rm F}/V_{\rm cyc}=1+w^2/4$ for $E_{\rm F}>V_0=wV_{\rm cyc}$ and $w>2$ with respect to the magnetic field, one obtains the known result[11]

$$B_{\rm crit}=\frac{2\pi V_0}{ea v_{\rm F}}\left[\frac{2}{1+\sqrt{1-(V_0/E_{\rm F})^2}}\right]^{1/2}. \tag{22}$$

B. Weak magnetic modulation

If a magnetic modulation is added to an electric one, very complicated interference effects may result. Only if the phase shift φ_s is zero or π, the resulting energy spectrum will be symmetric in ξ_0. Even in that case, the distribution of channeled states (regions II) in the E-ξ_0 diagram may become rather complicated, especially at low energies. For the mixed case channeled states may occur even if the modulation parameters w and s are not large enough to produce them for the pure electric and the pure magnetic modulation of these strengths. For weak magnetic modulation, $0<s<1$, and arbitrary strength of the electric modulation, channeled states can exist only below a certain energy, as in the pure electric modulation case.

For arbitrary phase shift φ_s the energy spectrum may be so asymmetric that in a certain energy range only channeled orbits exist which carry current in one (say the positive y) direction, but no channeled orbits carrying current in the opposite direction. Such a situation is presented in Fig. 11. The regions II, where channeled and drifting states coexist, is again calculated from Eqs. (19) and (20), i.e., from purely classical arguments.

If a 2DEG is subjected to such an asymmetric mixed modulation, it may happen that in the thermal equilibrium the channeled states carry a finite current. Of course, this current must be compensated by a corresponding opposite current carried by the drifting states.

For large magnetic modulation, $s>1$, and arbitrary electric modulation, the magnetic modulation dominates the energy spectra at large energies. The regions II with channeled states become more and more important, as can be seen from the pole structure of Eqs. (19) and (20). For very weak electric modulation, the results reduce to those of the pure magnetic modulation, apart from some peculiarities at very low energies, where additional regions of channeled orbits may exist.

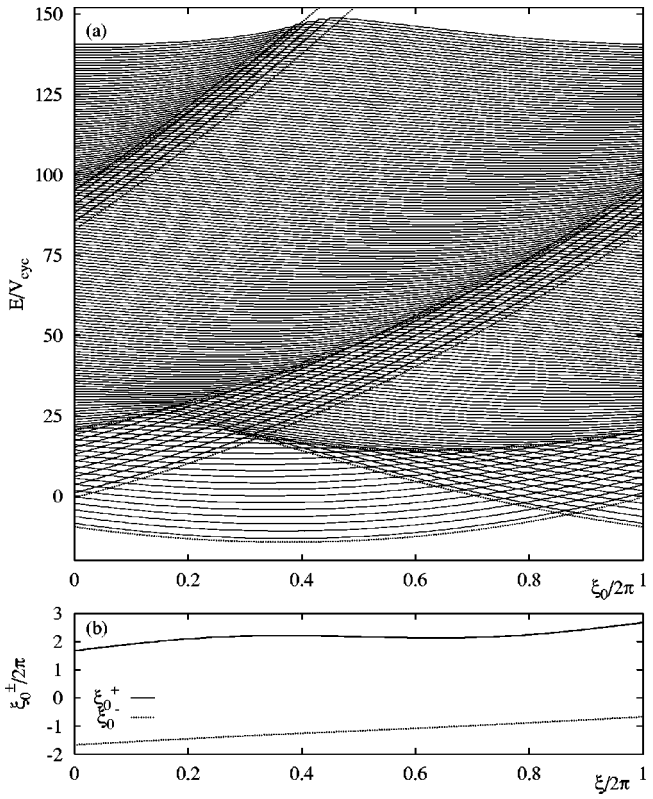

FIG. 11. (a) The first 175 Landau bands for combined magnetic and electric modulations. $B_0=0.1$ T and $a=800$ nm, so that $V_{\rm cyc}=0.213$ and $\alpha=0.16$. The modulation strengths are $s=0.8$ and $w=14.3$, the relative phase shift is $\pi/2$. (b) $\xi_0^{\pm}$ curves for $E/V_{\rm cyc}=110$. At this energy ξ_0^+ has local extrema, while there are none in ξ_0^-. Therefore all channeled orbits have negative velocities v_y.

In magnetically modulated systems prepared by the deposition of magnetic microstrips there is always an induced electric modulation due to the interface stress between the ferromagnets and the semiconductor.[6] The phase shift with respect to the magnetic modulation occurs when the external magnetic field is tilted.[21] Nevertheless, in the known experimental situations the stress potential amplitude is presumably much weaker than our bare potential.

V. SUMMARY AND DISCUSSION

We have discussed in detail the quantum electronic states and energy spectra $E_n(X_0)$ of a 2DEG in strong one-dimensional magnetic and electric superlattices, and in a nonvanishing average external magnetic field. By comparing the quantum results with the corresponding characteristics of the classical motion, we achieved a detailed and intuitive understanding of the energy spectra and eigenstates. We found that the complicated parts of the energy spectra (''regions II''), where branches with strong dispersion coexist with those of low dispersion, coincide with the areas in the $E-X_0$ diagram in which classically channeled orbits exist.

For a systematic investigation of the possible energy spectra and eigenstates, and of the corresponding types of classi-

cal trajectories, it is useful to exploit the scaling properties of the Hamiltonian. Then it is not necessary to vary independently all the basic model paramaters, i.e., the strengths B_m^0 and V_0 of magnetic and electric modulation, the modulation period a, and the average magnetic field B_0. If one uses suitable units for energy and length, $V_{\rm cyc}$ and $a/2\pi$, respectively, one obtains the same classical results and the same gross features of the energy spectra (the same position of the regions II), if one changes the *four* parameters B_m^0, V_0, a, and B_0 in such a manner that the *two* reduced modulation strengths $s=B_m^0/B_0$ and $w=V_0/V_{\rm cyc}$ remain constant. For different parameter sets with the same values of s and w, only the density of the energy bands is different in the plot of $E_n(X_0)/V_{\rm cyc}$ versus KX_0, not its overall appearance. This is illustrated by Figs. 7(a) and 8(a), for which the regions II coincide. The reason for this behavior is that, in these energy and length units, the effective potential is invariant under the scaling transformation $B_m^0 \rightarrow \gamma B_m^0$, $B_0 \rightarrow \gamma B_0$, $a \rightarrow \lambda a$, and $V_0 \rightarrow \gamma^2 \lambda^2 V_0$, for arbitrary positive γ and λ. To leave the quantum result exactly unchanged under a change of the four model parameters, one has to keep $\alpha=(l_0K)^4$ also unchanged. This is because only with the restriction $\lambda=1/\sqrt{\gamma}$ the kinetic-energy operator is also independent of the scaling parameter γ [see Eq. (8)]. Thus, in the suitable units, the exact quantum result depends only on *three* independent parameters instead of *four*, and the characteristic classical features depend only on *two*.

There is a close correspondence between the quantum states belonging to strong-dispersion branches of the energy spectrum and the classical channeled orbits. These orbits occur near lines of vanishing total magnetic field or near minima of the electric modulation potential and are restricted to individual side valleys of the effective potential. They are always restricted to a part of a single modulation period in x direction and represent a fast motion along (wavy) lines without self-intersections in the positive or negative y direction. The corresponding quantum states are also essentially confined to the same space region and belong to energy branches with strong dispersion. At a given value of the constant of motion X_0, channeled orbits exist in energy intervals bounded by adjacent relative minima and maxima of the effective potential, defining the bottom and top of the corresponding side valley. Plotting these classically defined extrema versus X_0, one obtains the boundaries of the regions II of the quantum energy spectrum. Classically, for each channeled orbit there exists a drifting orbit with the same constants of motion X_0 and E. These drifting orbits are self-intersecting trajectories which, for sufficiently large energy, extend over more than one modulation period in the x direction and drift slowly in the y direction. The corresponding quantum states belong to low-dispersion branches of the energy spectrum. Quantum mechanically, the channeled states do not appear at exactly the same energies as the drifting states, and they usually have a larger energy spacing than the latter, since they are confined to a narrower effective potential well.

We have demonstrated these features by model calculations based on simple harmonic modulation fields. Qualitatively the obtained results and the methods to derive them can easily be extended to more general modulation fields, containing higher harmonics. This will be necessary if the distance of the 2DEG from the sample surface is not much larger than the period of the surface structure creating the modulation.[21] Anharmonic effective modulation potentials may also result from nonlinear screening effects, even if the bare modulation potential is harmonic.[22,23]

We have also performed several additional calculations and consistency checks which are not documented in the main text. E.g., we have checked the equivalence of classical drift velocity and quantum group velocity beyond the analytically accessible case of very weak modulation fields. For some examples with strong modulation, we evaluated the quantum-mechanical group velocity along several energy bands $E_n(X_0)$ and compared the result with the drift velocity of the corresponding classical trajectories with the same energy and X_0 values. For most parts of the bands the two velocities agreed perfectly. A systematic deviation was observed only in parameter regimes where the classical trajectories are close to critical orbits, which have no quantum analog. Near the critical orbits the modulus of the classical drift velocity increases rather rapidly, whereas the quantum mechanical group velocity shows no anomaly.

We have also extended the band-structure calculations to very strong magnetic modulation ($B_m^0/B_0=20$). While at high energies a complicated superpositon of bands with steep and with flat dispersions, similar to that in Fig. 9(a), was obtained, the bands at low energies tend to cluster into groups separated by relatively large gaps. The low-energy part of the spectrum was already reminiscent of the spectrum for vanishing average magnetic field, where one obtains a one-dimensional Bloch energy spectrum for each value of $p_y=-eB_0X_0$.[16]

Concerning previous and forthcoming transport calculations, we conclude from the close correspondence of the quantum and the classical approach that at weak average magnetic fields the classical calculations are appropriate, provided the modulation fields are not too strong. For the very strong magnetic modulation mentioned in the Introduction, it may, however, happen that the energy-level spacing of channeled orbits exceeds the thermal energy k_BT in a regime where $\hbar\omega_0 \ll k_BT$. Then we would expect modulation-induced quantum effects in the positive-magnetoresistance regime at low B_0.

ACKNOWLEDGMENTS

We thank D. Pfannkuche for a critical reading of the manuscript. This work was supported by the German Bundesministerium für Bildung und Forschung (BMBF), Grant No. 01BM622. One of us (A.M.) is grateful to the Max-Planck-Institut für Festkörperforschung, Stuttgart for support and hospitality.

[1] D. Weiss, K. v. Klitzing, K. Ploog, and G. Weimann, Europhys. Lett. **8**, 179 (1989); also in *High Magnetic Fields in Semiconductor Physics II*, edited by G. Landwehr, Springer Series in Solid-State Sciences Vol. 87 (Springer-Verlag, Berlin, 1989), p. 357.
[2] R. R. Gerhardts, D. Weiss, and K. v. Klitzing, Phys. Rev. Lett. **62**, 1173 (1989).
[3] R. W. Winkler, J. P. Kotthaus, and K. Ploog, Phys. Rev. Lett. **62**, 1177 (1989).
[4] C. Zhang and R. R. Gerhardts, Phys. Rev. B **41**, 12 850 (1990).
[5] H. A. Carmona, A. K. Geim, A. Nogaret, P. C. Main, T. J. Foster, M. Henini, S. P. Beaumont, and M. G. Blamire, Phys. Rev. Lett. **74**, 3009 (1995).
[6] P. D. Ye, D. Weiss, R. R. Gerhardts, M. Seeger, K. von Klitzing, K. Eberl, and H. Nickel, Phys. Rev. Lett. **74**, 3013 (1995).
[7] S. Izawa, S. Katsumoto, A. Endo, and Y. Iye, J. Phys. Soc. Jpn. **64**, 706 (1995).
[8] P. D. Ye, D. Weiss, R. R. Gerhardts, and H. Nickel, J. Appl. Phys. **81**, 5444 (1997).
[9] C. W. J. Beenakker, Phys. Rev. Lett. **62**, 2020 (1989).
[10] P. H. Beton, E. S. Alves, P. C. Main, L. Eaves, M. Dellow, M. Henini, O. H. Hughes, S. P. Beaumont, and C. D. W. Wilkinson, Phys. Rev. B **42**, 9229 (1990).
[11] R. Menne and R. R. Gerhardts, Phys. Rev. B **57**, 1707 (1998).
[12] J. E. Müller, Phys. Rev. Lett. **68**, 385 (1992).
[13] Q. W. Shi and K. Y. Szeto, Phys. Rev. B **53**, 12 990 (1996).
[14] P. D. Ye, D. Weiss, R. R. Gerhardts, K. v. Klitzing, and S. Tarucha, Physica B **249-251**, 330 (1998).
[15] E. Hofstetter, J. M. C. Taylor, and A. MacKinnon, Phys. Rev. B **53**, 4676 (1996).
[16] I. S. Ibrahim and F. M. Peeters, Phys. Rev. B **52**, 17 321 (1995).
[17] A. Manolescu, S. D. M. Zwerschke, M. Nită, U. J. Gossmann, and R. R. Gerhardts, Physica B **256-258**, 375 (1998).
[18] P. Vasilopoulos and F. M. Peeters, Superlattices Microstruct. **7**, 393 (1990).
[19] F. M. Peeters and P. Vasilopoulos, Phys. Rev. B **47**, 1466 (1993).
[20] F. M. Peeters and A. Matulis, Phys. Rev. B **48**, 15 166 (1993).
[21] R. R. Gerhardts, Phys. Rev. B **53**, 11 064 (1996).
[22] U. Gossmann, A. Manolescu, and R. R. Gerhardts, Phys. Rev. B **57**, 1680 (1998).
[23] A. Manolescu and R. R. Gerhardts, Phys. Rev. B **56**, 9707 (1997).